

Dynamic analysis of water storage tank with rigid block at bottom

Ranjan Adhikary and Kalyan Kumar Mandal*

Department of Civil Engineering, Jadavpur University, Kolkata, India

(Received November 18, 2017, Revised January 19, 2018, Accepted January 22, 2018)

Abstract. The present paper deals with the finite element analysis of water tanks with rigid baffle. Fluid is discretized by two dimensional eight-node isoparametric elements and the governing equation is simulated by pressure based formulation to reduce the degrees of freedom in the domain. Both free vibration and force vibration analysis are carried out for different sizes and positions of block at tank bottom. The fundamental frequency depends on block height and it reduces with the increase of block height. The variation of hydrodynamic pressure on tank walls not only depends of the exciting frequency but also on the size and position of rigid block at tank bottom. The hydrodynamic pressure has higher value when the exciting frequency is equal and lower than the fundamental frequency of the water in the tank. Similarly, the hydrodynamic pressure increases with the increase of width of the block for all exciting frequencies when the block is at the centre of tank. The left and right walls of tank have experienced different hydrodynamic pressure when the block is placed at off-centre. However, the increase in hydrodynamic pressure on nearest tank wall becomes insignificant after a certain value of the distance between the wall and the rigid block.

Keywords: finite element analysis; rigid block; fundamental frequency; rigid surface; time history analysis

1. Introduction

The behavior of liquids in partially or fully filled containers against dynamic loading has always been concern for researchers and it remains a matter of interest in various fields of applied mathematics and engineering. Therefore, the economic design of a tank mainly depends upon the precise estimation of hydrodynamic pressure acting on these tanks wall.

Tung (1979) investigated hydrodynamic pressures and forces on submerged vertical cylindrical tanks under the action of harmonic ground excitations considering water to be incompressible and inviscid. Haroun and Tayel (1985) presented an analytical method for analyzing the axial stresses developed in elastic, cylindrical liquid storage anchored tank shell due to vertical excitation and concluded that the effects of vertical excitations were not significant compared to the effects of horizontal excitations because the steel cylindrical shells offer considerable resistance in the circumferential direction. The boundary integral method was used to calculate the hydrodynamic pressure distribution on a rigid submerged cylindrical storage tank subjected to horizontal or vertical harmonic ground excitations by Williams and Moubayed (1990). The liquid region in a

*Corresponding author, Associate Professor, E-mail: kkma_iitkgp@yahoo.co.in

cylindrical tank was solved using Rayleigh- Ritz procedure in combination with Lagrange's equation by Tang (1994) and shown that even though the fundamental natural frequency was quite sensitive to control the geometry of tanks. Pal *et al.* (2001) and Barrios *et al.* (2007) carried out a 3D finite element analysis of cylindrical rigid base container considering velocity potential as nodal variable. Celebi and Akyildiz (2002) investigated nonlinear 2D liquid sloshing characteristics of a partially filled rectangular tank considering liquid in this tank as homogeneous, isotropic, viscous, Newtonian with exhibit only limited compressibility. A coupled finite and boundary element formulation was developed to compute the natural frequencies of liquid filled tank-baffle system considering baffle as annular circular ring by Biswall *et al.* (2004). Similarly, Cho and Lee (2004, 2005) proposed a velocity-potential based finite element model to simulate the large amplitude liquid sloshing in two dimensional baffled tanks subjected to horizontal excitation. Chan and Kianoush (2006) proposed a simplified method using generalized SDOF system to determine the dynamic response of concrete rectangular liquid storage tanks considering only impulsive hydrodynamic pressure. Virella *et al.* (2008) investigated the influence of linear and nonlinear wave theory on the sloshing natural periods and their modal pressure distributions on rectangular tanks. After comparing the results, it was found that the nonlinearity does not have significant effects on the natural sloshing periods. Eswaran *et al.* (2009) carried out a numerical study based on volume of fluid technique with arbitrary-lagrangian-Eulerian formulation. Similarly, the seismic responses of a three dimensional cylinder using the Eulerian approach were determined by Firouz *et al.* (2011), Sygulski (2011), Ebrahimian *et al.* (2013). Kolaei *et al.* (2015) used boundary element to analyze the sloshing in an arbitrary shape tank against horizontal and vertical excitations. Finite difference approximation with the moving coordinate system was used to obtain hydrodynamic pressure by Akyildiz and Unal (2012). Jiang *et al.* (2014) and Cho and Kim (2016) investigated the movement of fluid and the pressure exerted by the fluid on walls of elliptical tank with different baffle configuration experimentally.

It is apparent from the literatures referred above that the fluid in the containers may be model either by finite element and boundary element. However, the finite element method based on Eulerian approach is advantageous. Again, the hydrodynamic pressure on tank walls is the major guiding factor for design of such tanks. The behavior of the fluid on tank or the hydrodynamic pressure acting on the tank walls may be controlled by introducing baffle or upliftment at tank bottom. In the present study, a pressure based finite element model is developed to obtain the free and force vibration responses of water in rectangular tanks with rigid block of different sizes and positions at bottom.

2. Theoretical formulations

The state of stress for a Newtonian fluid is defined by an isotropic tensor as

$$T_{ij} = -p\delta_{ij} + T'_{ij} \quad (1)$$

Where, T_{ij} is total stress, T'_{ij} is viscous stress tensor which depends only on the rate of deformation in such a way that the value becomes zero when the fluid is under rigid body motion or rest. The variable p is defined as hydrodynamic pressure whose value is independent explicitly on the rate of deformation and δ_{ij} is kronecker delta. For isotropic linear elastic material, the most

general form of T'_{ij} is

$$T'_{ij} = \lambda \Delta \delta_{ij} + 2\mu D_{ij} \quad (2)$$

Where, μ and λ are two material constants. μ is known as first coefficient of viscosity or viscosity and $(\lambda+2\mu/3)$ is second coefficient of viscosity or bulk viscosity. D_{ij} is the rate of deformation tensor and is expressed as

$$D_{ij} = \frac{1}{2} \left(\frac{\partial v_i}{\partial y_j} + \frac{\partial v_j}{\partial x_i} \right) \quad D = D_{11} + D_{22} + D_{33} \quad (3)$$

Thus, the total stress tensor becomes

$$T_{ij} = -p \delta_{ij} + \lambda \Delta \delta_{ij} + 2\mu D_{ij} \quad (4)$$

For compressible fluid, bulk viscosity $(\lambda+2\mu/3)$ is zero. Thus, Eq. (4) becomes

$$T_{ij} = -p \delta_{ij} - \frac{2\mu}{3} \Delta \delta_{ij} + 2\mu D_{ij} \quad (5)$$

If the viscosity of fluid is neglected, Eq. (5) becomes

$$T_{ij} = -p \delta_{ij} \quad (6)$$

Generalized Navier-Stokes equations of motion are given by

$$\rho \left(\frac{\partial v_i}{\partial t} + v_j \frac{\partial v_i}{\partial x_j} \right) = \frac{\partial T_{ij}}{\partial x_j} + \rho B_i \quad (7)$$

Where, B_i is the body force and ρ is the mass density of fluid. Substituting Eq. (6) in Eq. (7) the following relations are obtained.

$$\rho \left(\frac{\partial v_i}{\partial t} + v_j \frac{\partial v_i}{\partial x_j} \right) = \rho B_i - \frac{\partial p}{\partial x_i} \quad (8)$$

If u and v are the velocity components along x and y axes respectively and f_x and f_y are body forces along x and y direction respectively and if the convective terms are neglected, the equation of motion may be written as

$$\frac{1}{\rho} \frac{\partial p}{\partial x} + \frac{\partial u}{\partial t} = f_x \quad (9)$$

$$\frac{1}{\rho} \frac{\partial p}{\partial y} + \frac{\partial v}{\partial t} = f_y \quad (10)$$

Neglecting the body forces, Eqs. (9) and (10) become

$$\frac{1}{\rho} \frac{\partial p}{\partial x} + \frac{\partial u}{\partial t} = 0 \quad (11)$$

$$\frac{1}{\rho} \frac{\partial p}{\partial y} + \frac{\partial v}{\partial t} = 0 \quad (12)$$

The continuity equation of fluid in two dimensions is expressed as

$$\frac{\partial p}{\partial t} + \rho c^2 \left(\frac{\partial u}{\partial x} + \frac{\partial v}{\partial y} \right) = 0 \quad (13)$$

Where, c is the acoustic wave speed in fluid. Now, differentiating Eqs. (11) and (12) with respect to x and y respectively, the following relations are obtained.

$$\frac{1}{\rho} \frac{\partial^2 p}{\partial x^2} + \frac{\partial}{\partial x} \left(\frac{\partial u}{\partial t} \right) = 0 \quad (14)$$

$$\frac{1}{\rho} \frac{\partial^2 p}{\partial y^2} + \frac{\partial}{\partial y} \left(\frac{\partial v}{\partial t} \right) = 0 \quad (15)$$

Adding Eqs. (14) and (15) the following expression is finally arrived.

$$\frac{1}{\rho} \frac{\partial^2 p}{\partial x^2} + \frac{1}{\rho} \frac{\partial^2 p}{\partial y^2} + \frac{\partial}{\partial x} \left(\frac{\partial u}{\partial t} \right) + \frac{\partial}{\partial y} \left(\frac{\partial v}{\partial t} \right) = 0 \quad (16)$$

Differentiating Eq. (13) with respect to time, the following expression can be obtained.

$$\frac{\partial^2 p}{\partial t^2} + \rho c^2 \left[\frac{\partial}{\partial x} \left(\frac{\partial u}{\partial t} \right) + \frac{\partial}{\partial y} \left(\frac{\partial v}{\partial t} \right) \right] = 0 \quad (17)$$

Thus, from Eqs. (16) and (17), one can find the following expression

$$\frac{1}{\rho} \frac{\partial^2 p}{\partial x^2} + \frac{1}{\rho} \frac{\partial^2 p}{\partial y^2} - \frac{1}{\rho c^2} \frac{\partial^2 p}{\partial t^2} \quad (18)$$

Simplifying the Eq. (18), the equation for compressible fluid may be obtained

$$\nabla^2 p(x, y, t) = \frac{1}{c^2} \ddot{p}(x, y, t) \quad (19)$$

If, the compressibility of fluid is neglected the Eq. (19) will be modified as

$$\nabla^2 p(x, y, t) = 0 \quad (20)$$

The pressure distribution in the fluid domain may be obtained by solving Eq. (19) with the following boundary conditions. A typical geometry of tank-water system is shown in Fig. 1.

i) *At surface I*

Considering the effect of surface wave of the fluid, the boundary condition of the free surface is taken as

$$\frac{1}{g} \ddot{p} + \frac{\partial p}{\partial y} = 0 \quad (21)$$

ii) *At surface II and surface IV*

At water-tank wall interface, the pressure should satisfy

$$\frac{\partial p}{\partial n}(0, y, t) = \rho_f a e^{i\omega t} \quad (22)$$

Where $a e^{i\omega t}$ is the horizontal component of the ground acceleration in which, ω is the circular frequency of vibration and $i = \sqrt{-1}$, n is the outwardly directed normal to the element surface along the interface. ρ_f is the mass density of the fluid.

iii) *At surface III*

This surface is considered as rigid surface and thus pressure should satisfy the following condition

$$\frac{\partial p}{\partial n}(x, 0, t) = 0.0 \quad (23)$$

2.1 Finite element formulation

By using Galerkin approach and assuming pressure to be the nodal unknown variable, the discretized form of Eq. (19) may be written as

$$\int_{\Omega} N_{rj} \left[\nabla^2 \sum N_{ri} p_i - \frac{1}{c^2} \sum N_{ri} \ddot{p}_i \right] d\Omega = 0 \quad (24)$$

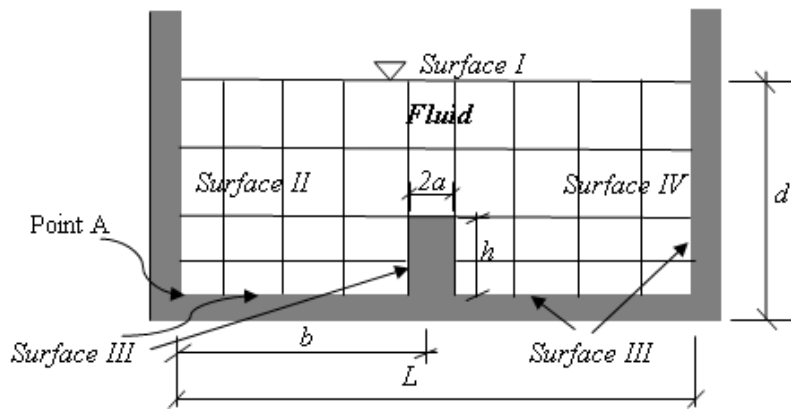


Fig. 1 Geometry of tank-water system

Where, N_{rj} is the interpolation function for the reservoir and Ω is the region under consideration. Using Green's theorem Eq. (24) may be transformed to

$$-\int_{\Omega} \left[\frac{\partial N_{rj}}{\partial x} \sum \frac{\partial N_{ri}}{\partial x} p_i + \frac{\partial N_{rj}}{\partial y} \sum \frac{\partial N_{ri}}{\partial y} p_i \right] d\Omega - \frac{1}{c^2} \int_{\Omega} N_{rj} \sum N_{ri} d\Omega \ddot{p}_i + \int_{\Gamma} N_{rj} \sum \frac{\partial N_{rj}}{\partial n} d\Gamma p_i = 0 \quad (25)$$

in which i varies from 1 to total number of nodes and Γ represents the boundaries of the fluid domain. The last term of the above equation may be written as

$$\mathbf{B} = \int_{\Gamma} N_{rj} \frac{\partial p}{\partial n} d\Gamma \quad (26)$$

The whole system of Eq. (5) may be written in a matrix form as

$$\bar{\mathbf{E}} \bar{\mathbf{P}} + \mathbf{G} \bar{\mathbf{P}} = \bar{\mathbf{F}} \quad (27)$$

Where,

$$\mathbf{E} = \frac{1}{C^2} \sum \int_{\Omega} \mathbf{N}_r^T \mathbf{N}_r d\Omega \quad (28)$$

$$\mathbf{G} = \sum \int_{\Omega} \left[\frac{\partial}{\partial x} \mathbf{N}_r^T \frac{\partial}{\partial x} \mathbf{N}_r + \frac{\partial}{\partial y} \mathbf{N}_r^T \frac{\partial}{\partial y} \mathbf{N}_r \right] d\Omega \quad (29)$$

$$\mathbf{F} = \sum \int_{\Gamma} \mathbf{N}_r^T \frac{\partial p}{\partial n} d\Gamma = \bar{\mathbf{F}}_I + \bar{\mathbf{F}}_{II} + \bar{\mathbf{F}}_{III} + \bar{\mathbf{F}}_{IV} \quad (30)$$

Here the subscript *I, II, III and IV* stand for different surface conditions. For surface wave, the Eq. (21) may be written in finite element form as

$$\bar{\mathbf{F}}_I = -\frac{1}{g} \mathbf{R}_f \bar{\mathbf{p}} \quad (31)$$

In which,

$$\mathbf{R}_f = \sum \int_{\Gamma_f} \mathbf{N}_r^T \mathbf{N}_r d\Gamma \quad (32)$$

At the *Surface II and Surface IV* if $\{a\}$ is the vector of nodal accelerations of generalized coordinates, $\{F_{II}\}$ and $\{F_{IV}\}$ may be expressed as

$$\bar{\mathbf{F}}_{II} \text{ and } \bar{\mathbf{F}}_{IV} = -\rho \mathbf{R}_{II} \vec{a} \text{ and } -\rho \mathbf{R}_{IV} \vec{a} \text{ respectively} \quad (33)$$

In which,

$$\mathbf{R}_{II} \text{ and } \mathbf{R}_{IV} = \sum \int_{\Gamma_{II \text{ and } IV}} \mathbf{N}_r^T \mathbf{N}_r d\Gamma \quad (34)$$

At Surface III

$$\vec{F}_{III} = 0 \quad (35)$$

After substitution all terms the Eq. (27) becomes

$$\mathbf{E}\vec{P} + \mathbf{A}\vec{P} + \mathbf{G}\vec{P} = \vec{F}_r \quad (36)$$

Where,

$$\mathbf{E} = \bar{\mathbf{E}} + \frac{1}{g} \mathbf{R}_I \quad (37)$$

$$\vec{F}_r = -\rho_f \mathbf{R}_{II} \vec{a} - \rho_f \mathbf{R}_{IV} \vec{a} \quad (38)$$

For any given acceleration at the fluid-structure interface, the Eq. (26) is solved to obtain the hydrodynamic pressure within the fluid.

2.2 Time history analysis of dynamic equilibrium equation

Dynamic equilibrium equation of fluid can be expressed as

$$\mathbf{E}\vec{P} + \mathbf{A}\vec{P} + \mathbf{G}\vec{P} = \vec{F}_r \quad (39)$$

In a linear dynamic system, these values remain constant throughout the time history analysis. The force vector is given by F_r . To obtain the transient response at time t_N , the time axis can be discretized into N equal time intervals ($t_N = \sum_{j=1}^N j\Delta t$). The choice of method for time-history

analysis is strongly problem dependent. Various direct time integration methods exist for time history analysis that are expedient for structural dynamics and wave propagation problem. Amongst these, the Newmark family of methods is most popular and is given by

$$\mathbf{P}_{j+1} = \mathbf{P}_j + \Delta t \dot{\mathbf{P}}_j + \frac{\Delta t^2}{2} [(1-2\nu)\ddot{\mathbf{P}}_j + 2\nu\ddot{\mathbf{P}}_{j+1}] \quad (40)$$

$$\dot{\mathbf{P}}_{j+1} = \dot{\mathbf{P}}_j + \Delta t [(1-\gamma)\ddot{\mathbf{P}}_j + \gamma\ddot{\mathbf{P}}_{j+1}] \quad (41)$$

Here, ν and γ are chosen to control stability and accuracy. It is evident from the literature that the integration scheme is unconditionally stable if $2\nu \geq \gamma \geq 0.5$

3. Numerical results

3.1 Validation of the proposed algorithm

In order to validate the proposed algorithm a bench marked problem is solved and results are

compared with the results obtained by Virella *et al.* (2008). The geometric and material properties of the tank are considered as follows: height of water in the tank = 6.10 m, length of tank = 30.5 m, so that ratio of height to length (d/l) = 0.2, density of water = 983 kg/m^3 , pressure wave velocity = 1451 m/s. Here, the interaction of fluid with in the tank and tank walls is neglected and the fluid is discretized by 4×8 (i.e., $N_h = 4$ and $N_v = 8$). The first three natural time periods of the tank fluid are listed and compared with those values obtained by Virella *et al.* (2008) in Table 1. The tabulated results show the accuracy of the present method.

3.2 Selection of suitable mesh size

To obtain a suitable mesh size, tank with following properties is considered. Water depth (d) = 1.6 m, length of tank (L) = 0.8 m acoustic speed (C) = 1440 m/sec, mass density of water (ρ) = 1000 kg/m^3 . The study is carried out for an exciting frequencies of $TC/d = 4000$ with amplitude of 1.0 g. The maximum pressure coefficient ($C_p = p / \rho * Amp * d$) for different mesh size are summarized in Table 2. From this table, it is observed that the maximum hydrodynamic pressure is converged when the horizontal division (N_h) is equal or higher than 4 and the ratio of vertical division to horizontal division (N_v/N_h) is equal to 1.0. However, for further numerical study, N_h is consider as 4 and the higher value (Fig. 1). The values of N_h and N_v are mention in respective examples.

3.3 Analysis of tank with rigid block at bottom

In this section, the responses of tank with different size of the rigid block at tank bottom are studied. The material properties for water with in the tank are follows: acoustic speed in water (C) = 1440 m/sec, mass density of water (ρ) = 1000 kg/m^3 . In the present study, tank walls and the tank bottom are considered as rigid. The water is discretized by 10×10 (i.e., $N_h = 10$ and $N_v = 10$) as obtained in the section 3.2. Similarly, for time history analysis the time step is considered as $T/32$.

3.3.1 Effect of the size of the rigid block on the frequency of tank

Here, the height and length of tank are considered as 13m and 30 m respectively. The sloshing frequencies of the tank are determined for different height of the block. Fig. 2(a) shows the variation of first three sloshing frequencies of the tank with different block heights. In this case the block is in the center on the tank and the width of the block is considered as 10 m. From the figure it is clear that all three sloshing frequencies decrease with the increase of the height of the block.

Table 1 First three natural time period of the tank fluid

Mode number	Natural time period in sec	
	Present Study	Virella <i>et al.</i> (2008)
1	8.46	8.38
2	3.94	3.70
3	2.89	2.78

Table 2 Convergence of hydrodynamic pressure coefficients (C_p) for different mesh size

Mesh Size ($N_h \times N_v$)	(1 × 2)	(2 × 1)	(2 × 2)	(3 × 1)	(3 × 2)	(3 × 3)	(4 × 2)	(4 × 3)	(4 × 4)	(4 × 6)
N_v/N_h	2	0.5	1	0.33	0.67	1	0.5	0.75	1	1.5
Pressure coefficient ($P/(apd)$)	1.8654	1.6293	1.9792	1.9108	1.9861	2.0568	2.0761	2.1274	2.2792	2.2792

The variations of these frequencies are quite different. The first and third frequencies shows almost similar trend and the reduction is more compare to the second frequency. However, the second frequency experiences lower reduction with the increase of the block highly. The different mode shapes for water in the tank with rigid block at tank bottom are shown in Fig. 2(b).

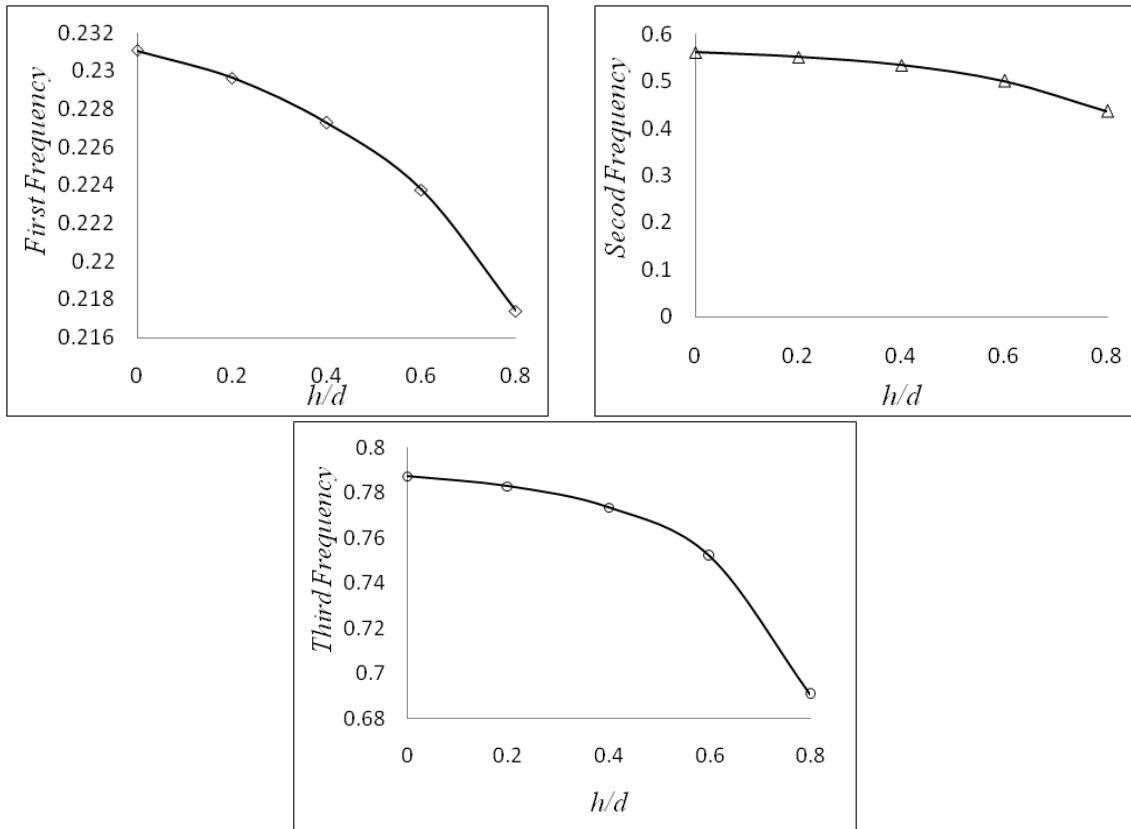


Fig. 2a Variation of sloshing frequency for various block height

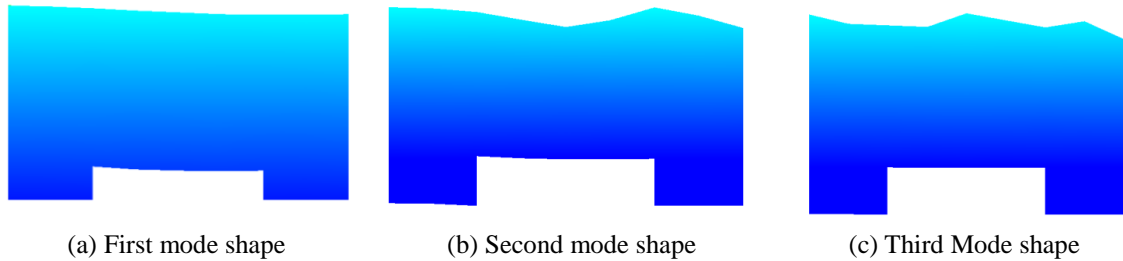


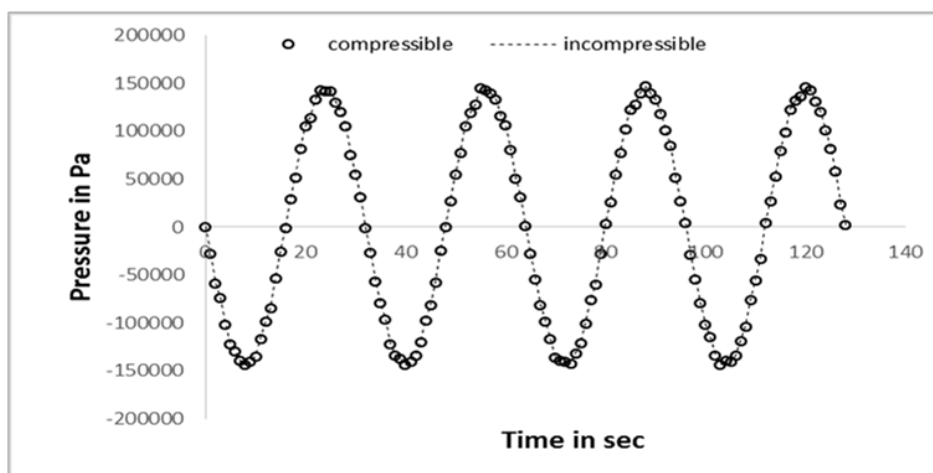
Fig. 2b Different modes of water in tank

3.3.2 Comparison of responses for compressible and incompressible

In this section, the water is considered as compressible as well as incompressible. Geometry of tank is as considered in section 3.3.1. For compressible fluid, the material properties as mentioned in section 3.2 are considered. This study is carried out for tank with block at the bottom at the centre. Here, the sinusoidal acceleration of three different frequencies such as $TC/d=36720$, 3672 and 367.2 and an amplitude of 1.0 m/sec^2 are considered as eternal excitation. Figs. 3-5 show the comparison of pressure for compressible and incompressible fluid at point-A (Fig. 1) due to different exciting frequencies. From these figures it is clear that the pressure at point A does not change with the consideration of compressibility of water. Hence the rest of the study is carried out without considering the compressibility effect of the water.

3.3.3 Analysis of rectangular tank with rigid block at centre.

In this section, the effect of rigid block at the bottom of the tank is studied. Here, the rigid block is considered at the centre of the tank. The studied is carried out for different width and height of the block. The geometry and material property of the tank are as follows (Fig. 1): Length (L) = 30 m, depth of water (d) = 13 m. Density of fluid is considered as 1000 Kg/m^3 . The responses of tanks are calculated against sinusoidal acceleration of three different frequencies.

Fig. 3 Pressure at point A of tank with rigid block at the centre for $TC/d=36720$

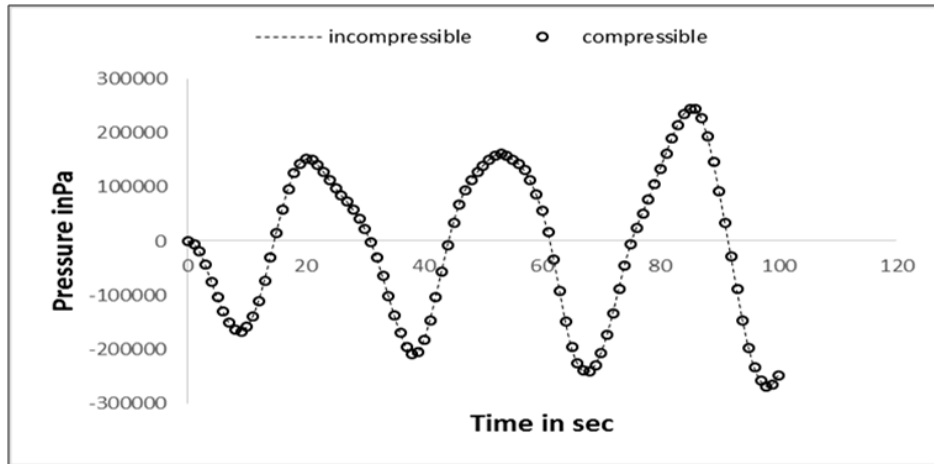


Fig. 4 Pressure at point A of tank with rigid block at the centre for $TC/d=3672$

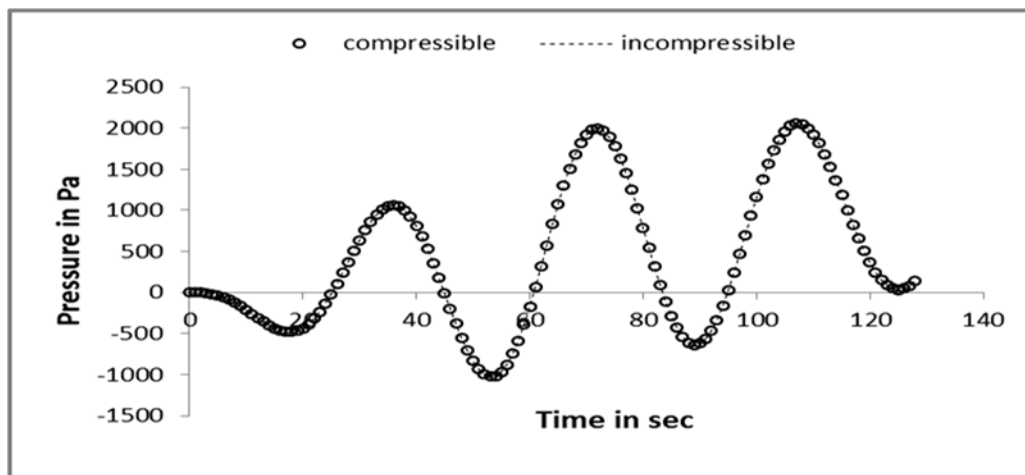


Fig. 5 Pressure at point A of tank with rigid block at the centre for $TC/d=367.2$

Figs .6-8 show comparison of hydrodynamic pressure at point A (Fig. 1) for block width of 6 m and different heights. It is clear from the figure that the hydrodynamic pressure increases with the increase of the block height when exciting frequency is equal or less than the fundamental frequency of tank. However, this increase in hydrodynamic pressure is more when the exciting frequency is equal to the fundamental frequency of the tank. Meanwhile, the tank wall experiences comparatively less hydrodynamic pressure for other to frequency and it gets reduced with the height of the block. Again, the study is carried out for block width of 18 m. For block with of 18m, the change in hydrodynamic pressure with the increase of height of the block is not significant when the exciting frequency is less than fundamental frequency of the tank (Fig. 9). However, this change remains significant for the case when exciting frequency equal and greater than the fundamental frequency of the tank (Figs.10 and 11).

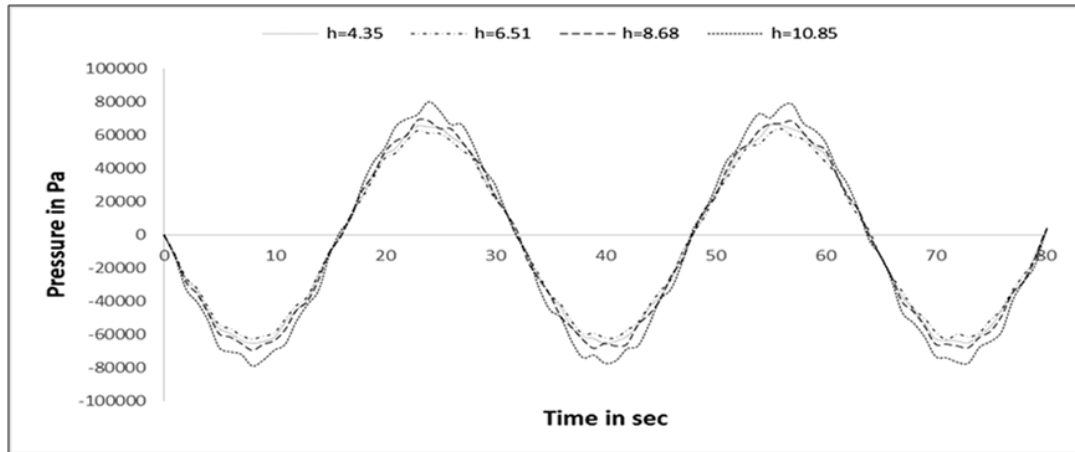


Fig. 6 Pressure at point A of tank with rigid block of width 6m for $TC/d=36720$

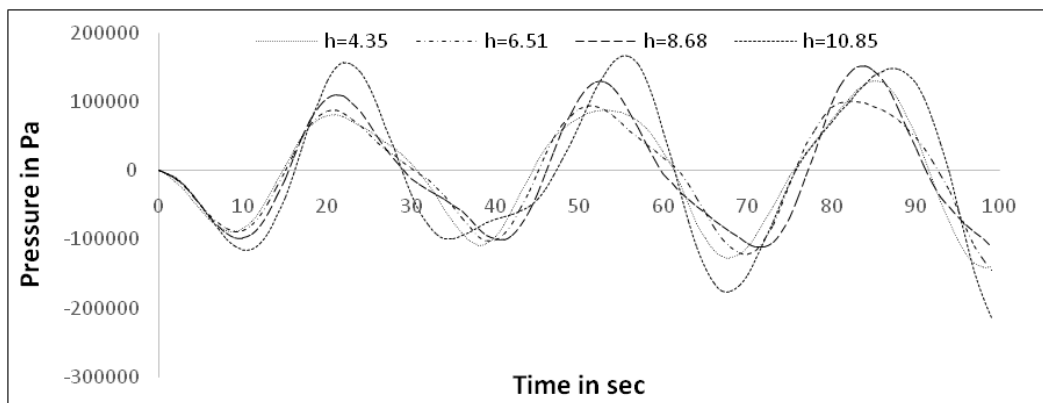


Fig. 7 Pressure at point A of tank with rigid block of width 6m for $TC/d=3672$

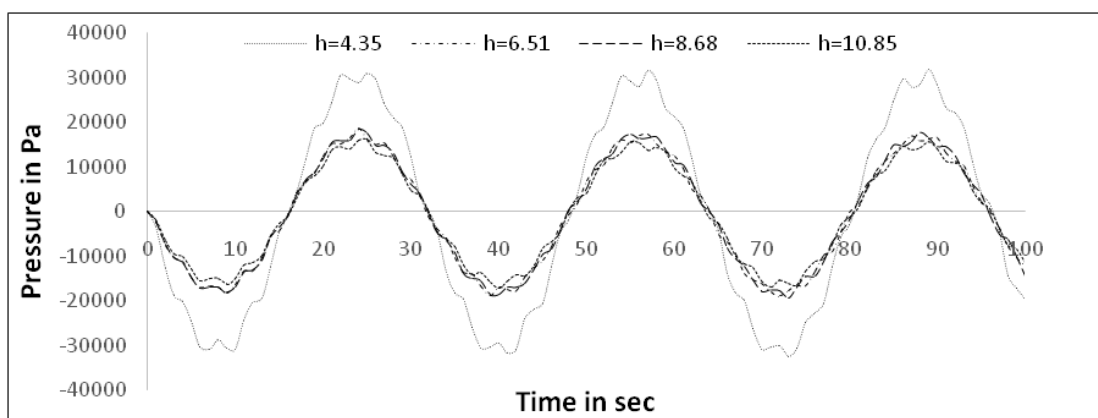


Fig. 8 Pressure at point A of tank with rigid block of width 6m for $TC/d=367.2$

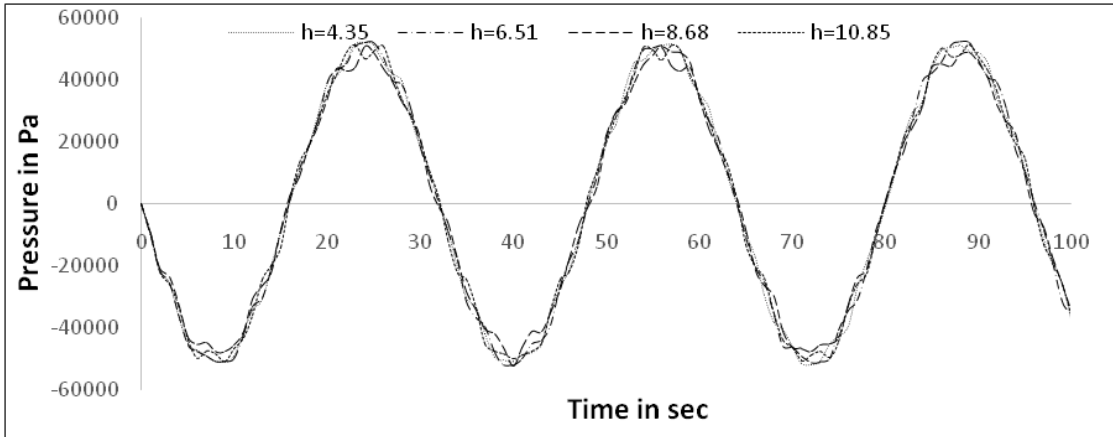


Fig. 9 Pressure at point A of tank with rigid block of width 18m for $TC/d=36720$

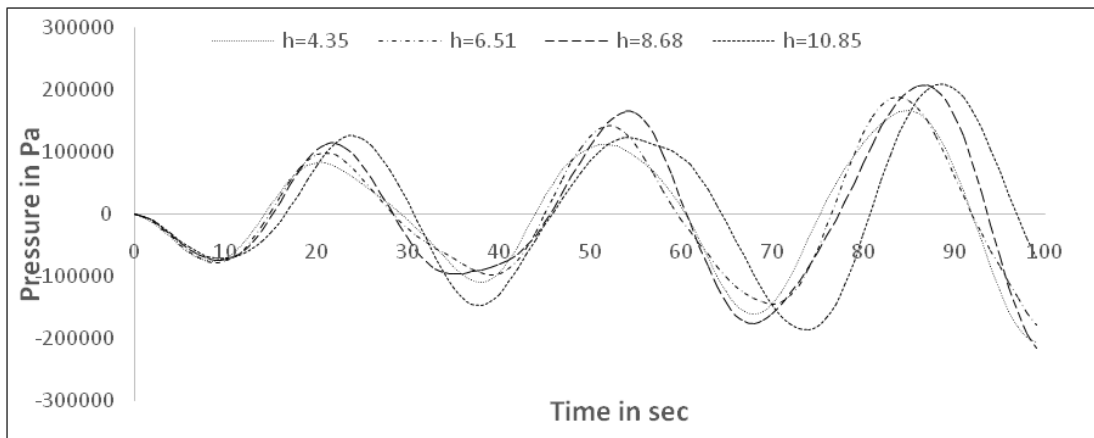


Fig. 10 Pressure at point A of tank with rigid block of width 18m for $TC/d=3672$

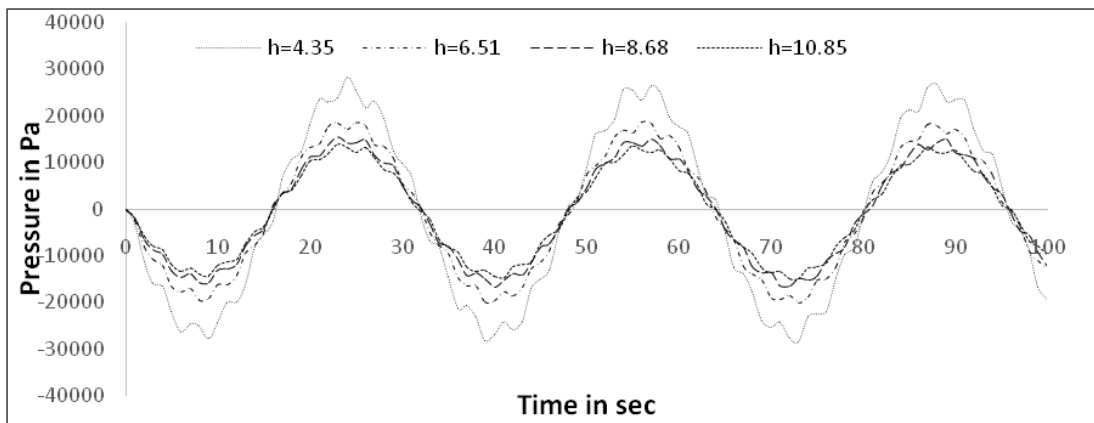


Fig. 11 Pressure at point A of tank with rigid block of width 18m for $TC/d=367.2$

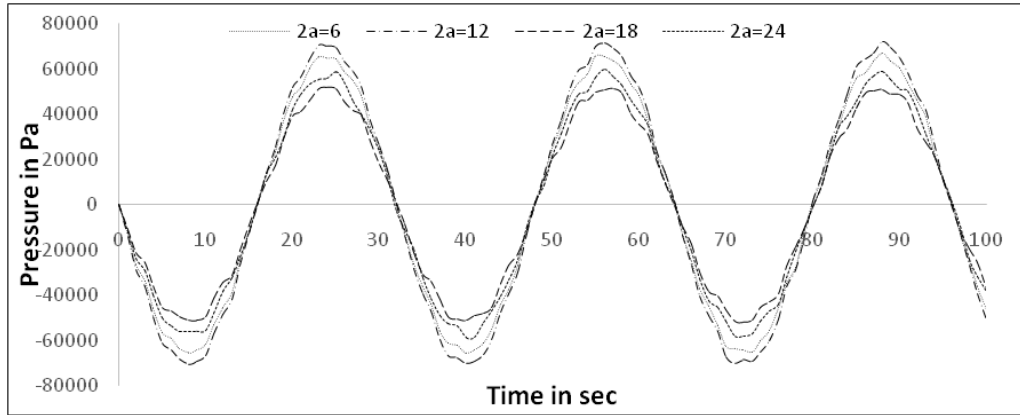


Fig. 12 Pressure at point A of tank with rigid block of height 4.35m for $TC/d=36720$

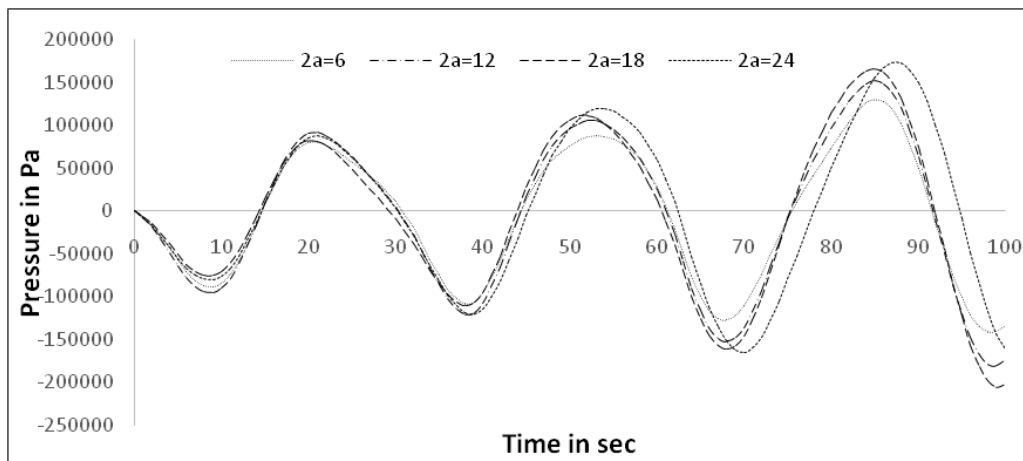


Fig. 13 Pressure at point A of tank with rigid block of height 4.35m for $TC/d=3672$

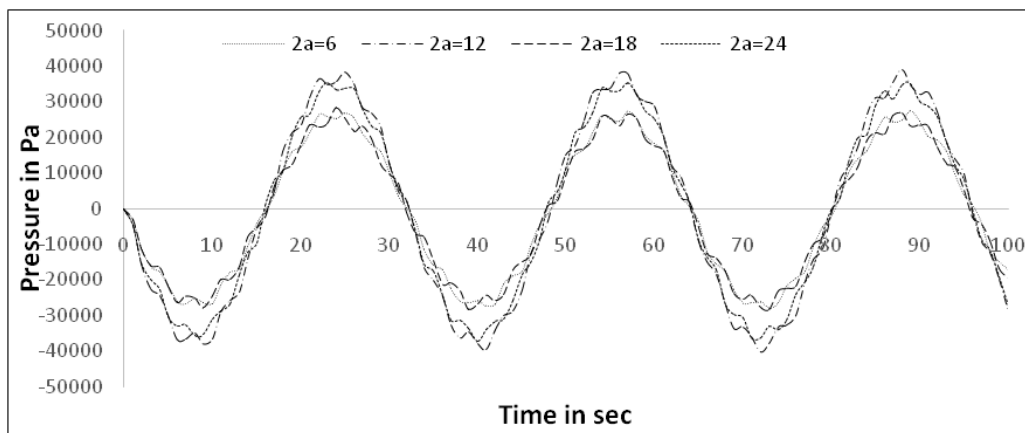


Fig. 14 Pressure at point A of tank with rigid block of height 4.35m for $TC/d=367.2$

The study is further extended for block with constant height and different width (Figs. 12-14). The maximum hydrodynamic pressure occurs when the width of the block is 12 m and the exciting frequency is less than the fundamental frequency of the tank (Fig. 12) and the variation of hydrodynamic pressure with the width of the block does not follow a regular pattern. Similar trend is observed when the fundamental frequency is greater than the fundamental frequency of the tank (Fig. 13). However, the hydrodynamic pressure at point A (Fig. 1) increases continuously with the increase of width of the block in case of frequency equal to the fundamental frequency of the water tank (Fig. 14).

3.3.4 Analysis of rectangular tank with rigid block at off-centre

Here an attempt has been taken to study the influence of the position of the rigid block at tank bottom. The geometry and material properties are as considered in section 3.3.3. As the response of the tank depends on the exciting frequency, the study is extended for sinusoidal excitation of three different frequencies, i.e., lower, greater and equal to the fundamental frequency of tank. For all the cases amplitude of the excitation is considered to be gravitational acceleration. From Fig. 15, it is clear that the hydrodynamic pressure at point A is almost independent to the position of the block when the exciting frequency is less than the fundamental frequency of the tank. However, the hydrodynamic pressure increases as the rigid block moves towards the left wall for the case when exciting frequency is equal and greater than the fundamental frequency of the tank (Figs. 16-17) and the maximum pressure is obtained for $b/l=0.2$.

It is further examined the variation of hydrodynamic pressure at point A (Fig. 1) with b/l ratio for different block heights. Here the heights of the block are considered as 6.51 m. Fig. 15-17 shows the variation of hydrodynamic pressure at point A (Fig. 1) against the sinusoidal acceleration of three different frequencies, i.e., $TC/d=367.2$, 3672 and 36720. Variation of hydrodynamic pressure with different b/l ratios depends on the exciting frequencies. Hydrodynamic pressure at point A increase with the increase of b/l ratio for exciting frequency less than the fundamental frequency of reservoir.

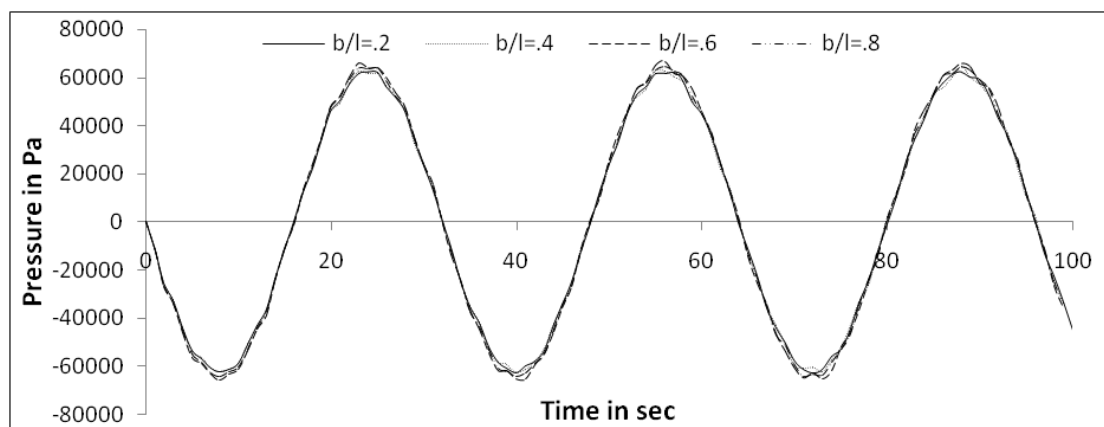


Fig. 15 Pressure at point A of tank with rigid block of height 4.35m for $TC/d=36720$

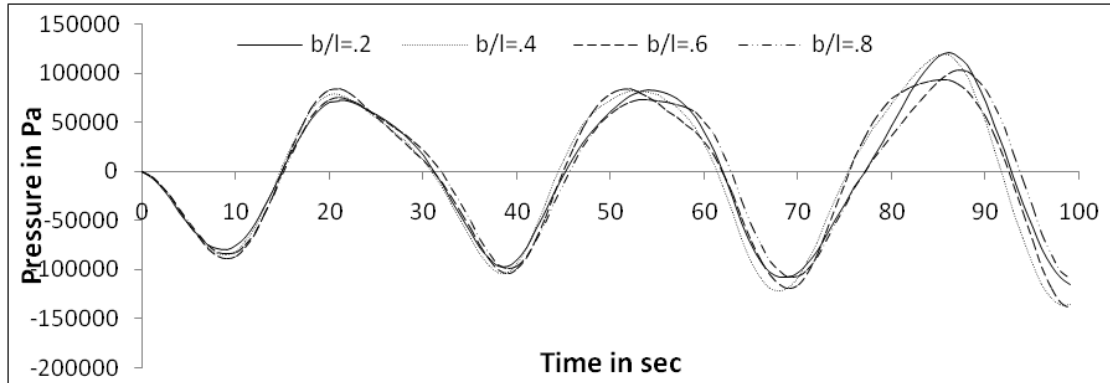


Fig. 16 Pressure at point A of tank with rigid block of height 4.35m for $TC/d = 367.2$

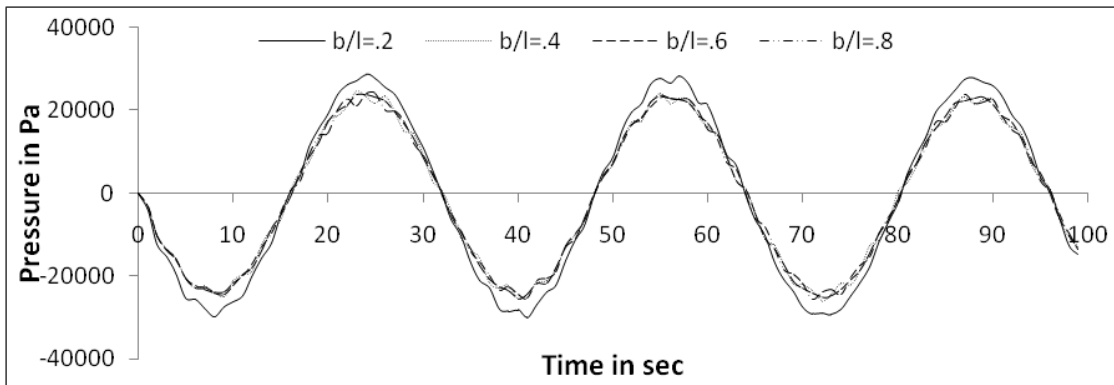


Fig. 17 Pressure at point A of tank with rigid block of height 4.35m for $TC/d = 367.2$

However, this increase in pressure is very less almost negligible after a certain b/l ratio, here it is 0.6 (Figs. 18). For exciting frequency equal to the fundamental frequency of reservoir, hydrodynamic pressure exerted on left wall increases as the b/l ratio increases for all widths of the rigid block and the increase in hydrodynamic pressure at point A becomes more prominent for comparatively higher block width (Fig. 19). On the other hand the hydrodynamic pressure on the left tank wall decreases continuously with the increases of b/l ratio (Fig. 20). In this case, the maximum and minimum hydrodynamic pressure occurs at b/l ratio equal to 0.2 and 0.8 respectively.

The hydrodynamic pressure along the length of the tank walls i.e., left and right walls for different block widths and exciting frequencies are plotted in Figs. 21 and 22. From these figures, it is clear that the hydrodynamic pressure on left wall decreases with b/l ratio whereas the pressure on right wall goes on increasing with the values of b/l ratio. These changes in hydrodynamic pressure on left and right walls increase with the increase of the width of the rigid block. The distribution of hydrodynamic pressure along the walls of the tank changes continuously with the change of the exciting frequencies. The pressure on both the walls increases with the increase of block height for a particular b/l ratio.

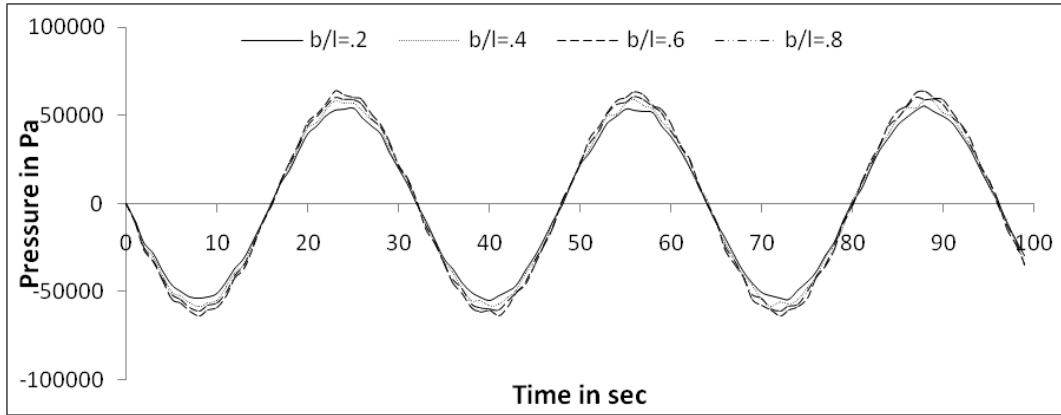


Fig. 18 Pressure at point A of tank with rigid block of height 6.51m for $TC/d = 36720$

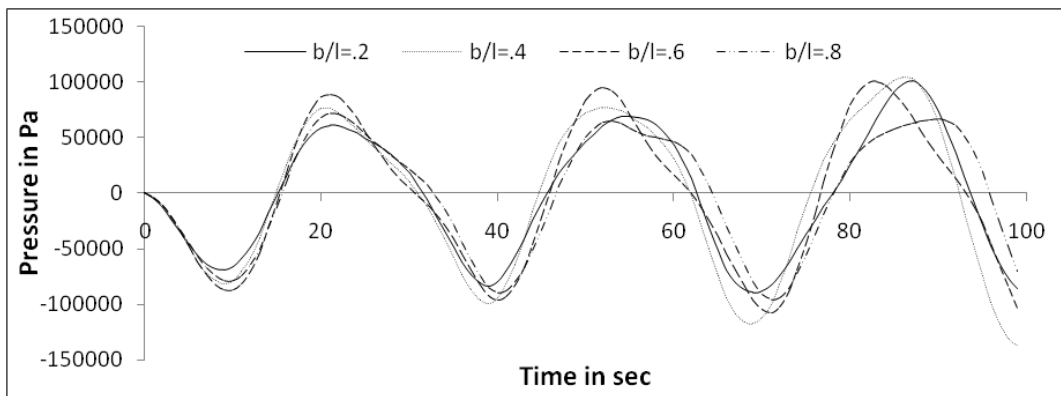


Fig. 19 Pressure at point A of tank with rigid block of height 6.51m for $TC/d = 3672$

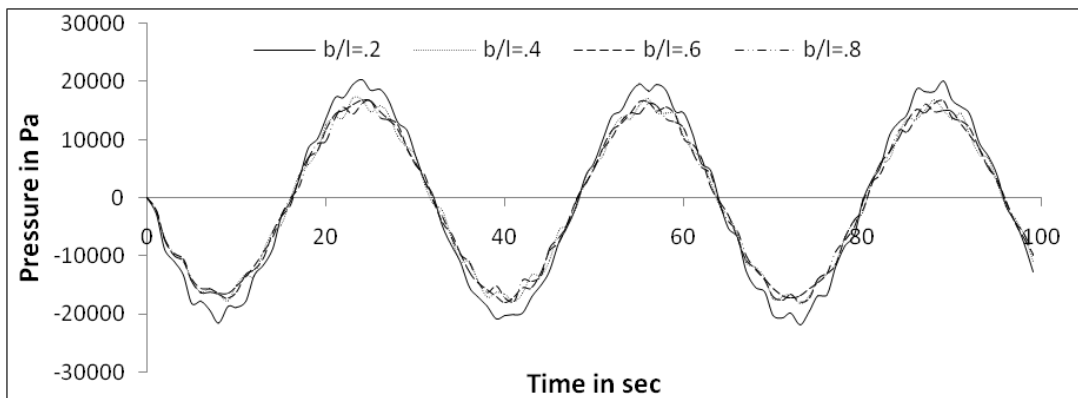


Fig. 20 Pressure at point A of tank with rigid block of height 6.51m for $TC/d = 367.2$

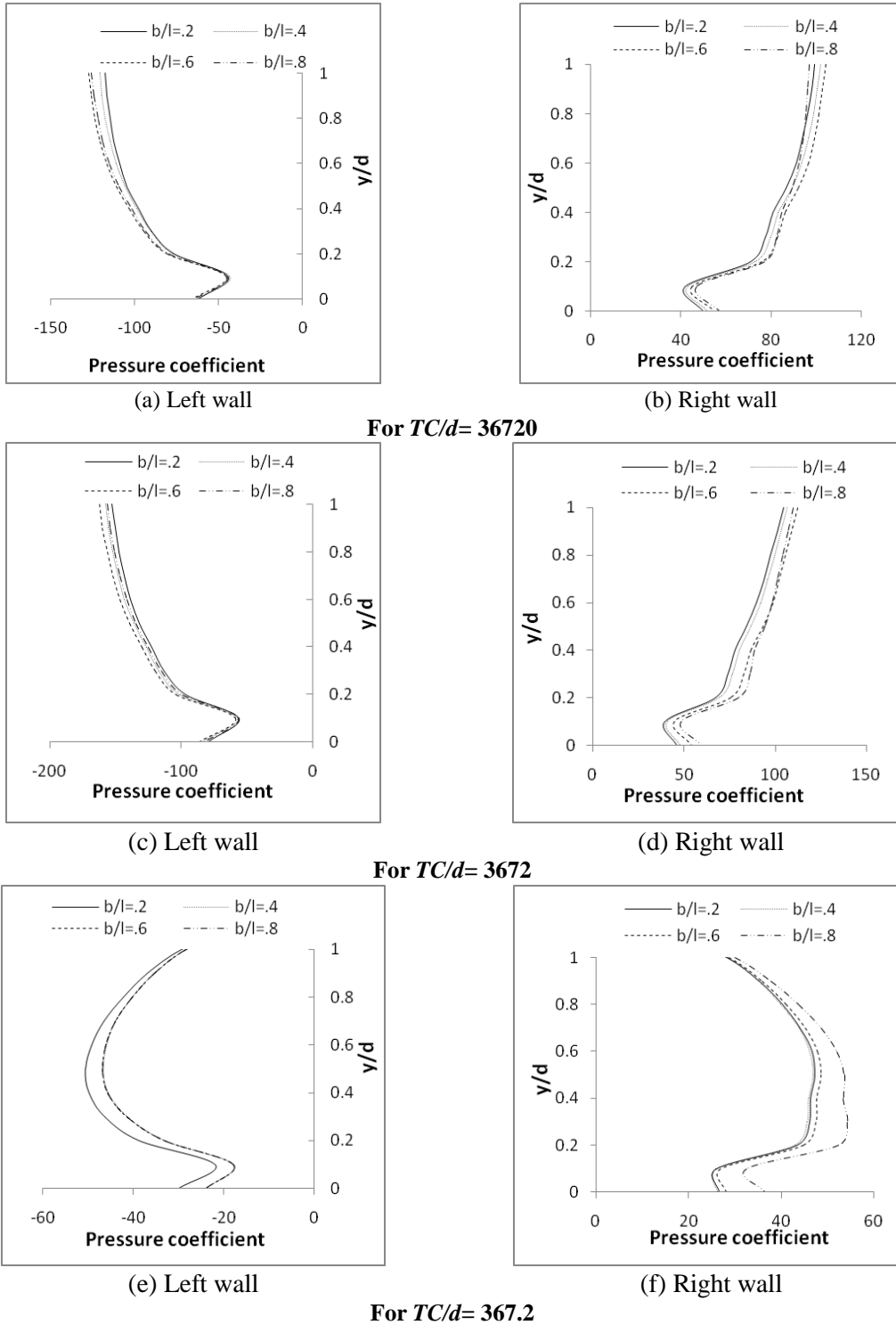


Fig. 21 Variation of hydrodynamic pressure along the tank walls for block height 4.35m

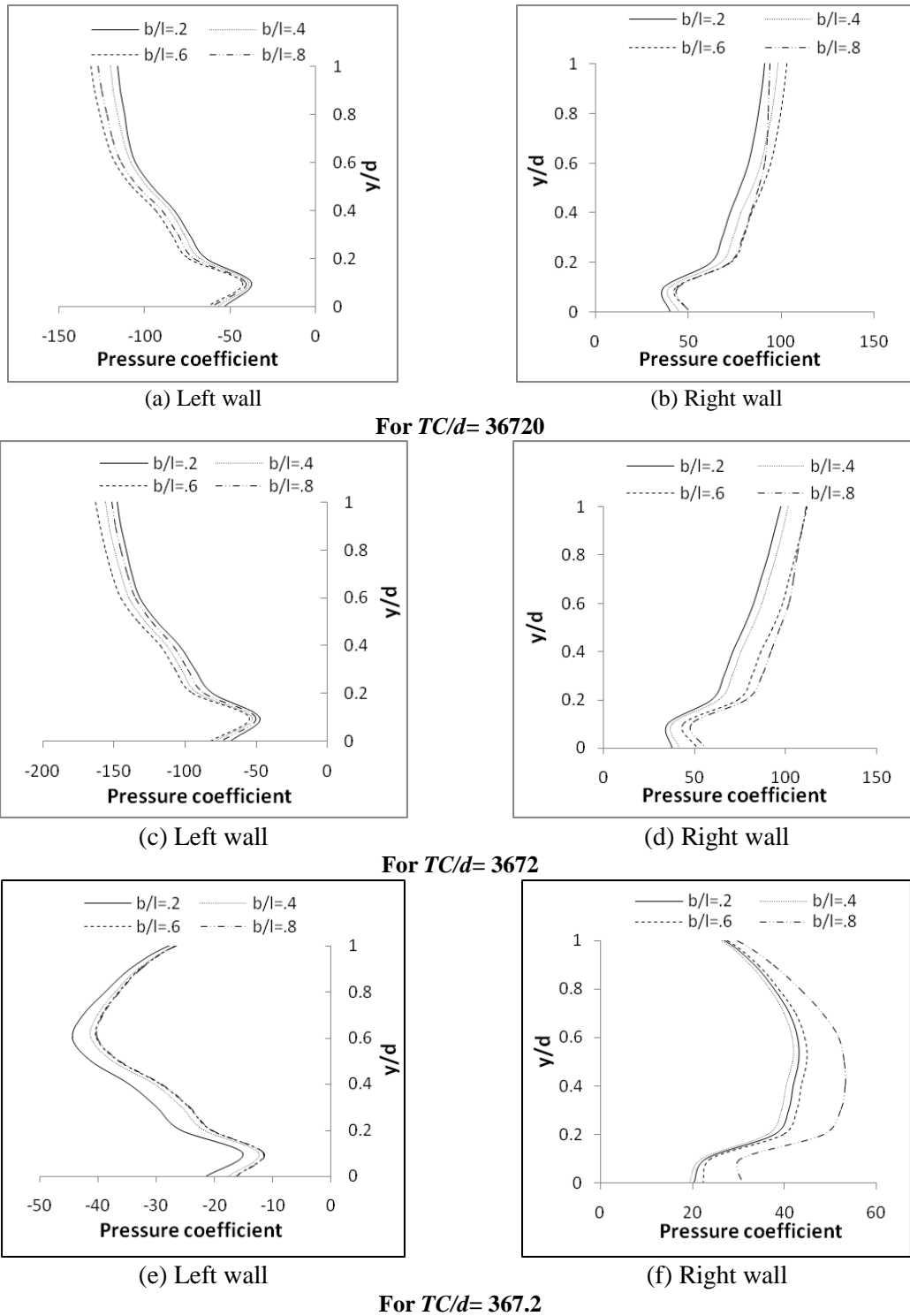


Fig. 22 Variation of hydrodynamic pressure along the tank walls for block height 6.51 m

4. Conclusions

The characteristics of hydrodynamic pressures on the wall of a rectangular water tank with rigid block of different sizes are studied. The water in the tank is considered to be linearly compressible as well as incompressible. A pressure based finite element method is used to simulate the dynamic behavior of water in tanks. The fundamental frequency of the tank water decreases with the increase of the block height. However, the variations are different for different fundamental frequencies. The first and third frequencies shows almost similar trend and the reduction is more compare to the second frequency. However, the second frequency has lower reduction with the increase of size of blocks. The hydrodynamic pressure on tank wall depends on the exciting frequencies. The hydrodynamic pressure has comparatively higher value when the exciting frequency is equal and lower than the first fundamental frequency of the water in the tank. The hydrodynamic pressure increases with the increases of width of the block for all exciting frequencies when the block is at the centre of tank. The similar trend of hydrodynamic pressure is observed for different height of block at exciting frequency equal and less than the fundamental frequency of the reservoir and this is due to the reduction of fundamental frequency with the height of the block. However, the trend becomes reverse for frequency greater than the fundamental frequency of reservoir. The left and right walls of tank experienced different hydrodynamic pressure when the block is placed at off-centre and its magnitude also depends on the exciting frequency and the position of the block. The pressure on the wall will be more when the block is closer to that wall. However, the increase in the pressure becomes insignificant after a certain value of the distance between the wall and the rigid block.

References

- Akyildiz, H. and Unal, E. (2012), "A numerical study of the effects of the vertical baffle on liquid sloshing in two dimensional rectangular tank", *J. Sound Vib.*, **331**(1), 41-52.
- Barrios, H.H., Zavoni, E.H. and Aldama-Rodriguez A.A. (2007), "Nonlinear sloshing response of cylindrical tanks subjected to earthquake ground motion", *Eng. Struct.*, **29** (12), 3364-3376.
- Biswal, K.C., Bhattacharyya, S.K. and Sinha P.K. (2006), "Non-linear sloshing in partially liquid filled containers with baffles", *Int. J. Numer. Method. Eng.*, **68** (4), 317-337.
- Celebi, M.S. and Akyildiz H. (2002), "Nonlinear modeling of liquid sloshing in a moving rectangular tank", *J. Ocean Eng.*, **29**(12), 1527-1553.
- Chen, J.Z. and Kianoush, M.R. (2006), "Effect of vertical acceleration on response of concrete rectangular liquid storage tanks", *Eng. Struct.*, **28**(5), 704-715.
- Cho, R.J. and Lee, H.W. (2005), "Finite element analysis of resonant sloshing response in 2-D baffled tank", *J. Sound Vib.*, **288**(5), 829-845.
- Cho, J.R. and Lee, H.W. (2004), "Numerical study on liquid sloshing in baffled tank by nonlinear finite element method", *J. Comput. Method. Appl. M.*, **193**(23), 2581-2598.
- Cho, H.I. and Kim, H.M. (2016), "Effect of dual vertical porous baffles on sloshing reduction in a swaying rectangular tank", *Ocean Eng.*, **126**, 364-373.
- Ebrahimian, M., Noorian, M.A. and Haddadpour, H. (2013), "A successive boundary element model for investigation of sloshing frequencies in axis-symmetric multi-baffled containers", *Eng. Anal. Bound. Elem.*, **37**(2), 383-392.
- Eswaran, M., Saha, U.K. and Maity, D. (2009), "Effect of baffles on a partially filled cubic tank: Numerical simulation and experimental validation", *Comput. Struct.*, **87**(4), 198-205.
- Haroun, M.A. and Tayel, M.A. (1985), "Axisymmetrical vibration of tanks-analytical", *J. Eng. Mech.* -

- ASCE., **111**(3), 346-358.
- Jiang, M., Bing, R., Guoyu, W. and Young-xue, W. (2014), "Laboratory investigation of the hydro-elastic effect on liquid sloshing in rectangular tanks", *J. Hydrodynamics*, **26**, 751-761.
- Kilic, A.S. (2009), "Simulation of Sloshing Effects in Cylindrical Tanks and Evaluation of Seismic Performance", *Lifeline Earthquake Engineering in a Multihazard Environment*, ASCE.
- Kolaei, A., Rakheja, S. and Richard, M.J. (2015), "Three-dimensional dynamic liquid slosh in partially-filled horizontal tanks subject to simultaneous longitudinal and lateral excitations", *Eur. J. Mech. B- Fluids.*, **53** (1), 251-263.
- Pal, N.C., Bhattacharyya, S.K. and Sinha R.K. (2001), "Experimental Investigation of Slosh Dynamics of Liquid-filled Containers", *Exp. Mech.*, **41**(1) 63-69.
- Sygulski, R. (2011), "Boundary element analysis of liquid sloshing in baffled tanks", *Eng. Anal. Bound. Elem.*, **35**(8), 978-983.
- Tang, Y. (1994), "Free vibration analysis of tank containing two liquids", *J. Struct. Eng. - ASCE.*, **120**(3), 618-636.
- Tung, C.C. (1979), "Hydrodynamic forces on submerged vertical circular cylindrical tanks underground excitation", *J. Appl. Ocean Res.*, **275**(1), 75-78.
- Virella, J.C., Prato, C.A. and Godoy, L.A. (2008), "Linear and nonlinear 2D finite element analysis of sloshing modes and pressures in rectangular tanks subject to horizontal harmonic motions", *J. Sound Vib.*, **312**(6), 442-460.
- Williams, A.N. and Moubayed, W.I. (1990), "Earthquake-induced hydrodynamic pressures on submerged cylindrical storage tanks", *Ocean Eng.*, **17**(3), 181-199.